Lasers in Surgery and Medicine 25:69–78 (1999)

Investigations on Acoustic On-Line Monitoring of IR Laser Ablation of Burned Skin

Kester Nahen, MS* and Alfred Vogel, PhD

Medical Laser Center Lübeck, 23562 Lübeck, Germany

Backround and Objective: **In burn surgery necrotic tissue has to be removed prior to grafting. Tangential excision causes high blood loss and destruction of viable tissue. Pulsed infrared laser ablation can overcome both problems because of its high precision and the superficial coagulation of the remaining tissue. We investigated the ablation noise to realize an acoustic feedback system for a selective removal of necrotic tissue.**
Materials and Methods: **We studied free-running Er:YAG laser ablation of gelatin and burned skin. Schlieren laser flash photography was used to investigate the ablation dynamics generating the ablation noise. Acoustic signals were detected by a condenser microphone and a piezoelectric airborne transducer. Tissue discrimination was based on the evaluation of the normalized acoustic energy.**
Results: **The ablation noise is mainly generated by shock wave emission and fast vaporization during the first part of the laser pulse. Frequency components of the ablation noise above 200 kHz are only detectable with the piezoelectric transducer. The normalized acoustic energy differs significantly between gelatin samples of different water content and between necrotic and vital tissue.**
Conclusions: **Large bandwidth transducers are essential for an acoustic on-line monitoring of free-running Er:YAG laser ablation of burned skin. The normalized acoustic energy is a suitable parameter for the discrimination between necrotic and vital tissue. Lasers Surg. Med. 25:69–78, 1999.**

Key words: acoustic transients; burn debridement; acoustic feedback

INTRODUCTION

For the treatment of severe burns the necrotic tissue has to be removed to minimize toxic effects on the patients organism and to prepare a vascularized burn wound for skin grafting. The vital tissue underlying the zone of necrosis needs to be preserved as well as possible because dermal components are essential for a fast skin graft take and a high stability of the graft. Today, tangential excision is the standard treatment for deep dermal burns [1]. In tangential burn eschar excision, tissue is shaved until pinpoint bleeding is observed and a viable base is reached. This treatment goes along with a high amount of blood loss and a considerable loss of viable tissue limiting the tangential method to burns of less than 30% of total body surface area [2].

The burn debridement can be improved by using pulsed laser tissue ablation. Pulsed infrared lasers like the CO_2 and Er:YAG laser allow a precise and effective removal of necrotic tissue [2,3]. The superficial coagulation of the remaining

Contract grant sponsor: The State of Schleswig-Holstein, Germany.

*Correspondence to: Kester Nahen, Medical Laser Center Lübeck, Peter-Monnik-Weg 4, D-23562 Lübeck, Germany. E-mail: nahen@mll.mu-luebeck.de

Accepted 4 March 1999

tissue prevents bleeding during the treatment and does not appreciably affect skin graft take [3,4]. The consumption of blood conserves is thereby reduced and larger burn areas can be treated during one operation improving the prognosis of the patient. For a fast and selective debridement of large area burns the laser beam has to be scanned and controlled by a system that differentiates between necrotic and vital tissue. By this way, unnecessarily deep excisions can be avoided.

The monitoring system for tissue discrimination should be a noncontact technique working in real time during the tissue ablation. Our approach is to realize a feedback system based on the analysis of the ablation noise. The ablation noise is generated by the explosive evaporation of the tissue water, which is the main chromophore for the infrared laser wavelengths used. Different degrees of hydration in different tissue layers as well as differences in the strength of the tissue matrix should thus be reflected in the acoustic signal.

Although pulsed laser ablation has been studied for a long period of time, only a few investigations evaluated the potential of the ablation noise analysis for material discrimination and process control. Leung et al. [5], Grad and Mozina [6], and Stauter et al. [7] investigated Excimer and Nd:YAG laser ablation of ceramics and found a correlation between the ablation rate and the amplitude and energy of the acoustic signal. Acoustic measurements during tissue ablation were only performed by Bende and Jean [8,9] by using Excimer laser pulses and by Altshuler et al. [10,11] and Grad et al. [12] by using a free-running Er:YAG laser for the ablation of dental materials. The possibility of a photoacoustic discrimination of burned skin layers or other soft tissues has not been investigated to date. One would expect that the ablation dynamics during the removal of necrotic and vital tissue differs because of the different biomechanical properties and water content of the two layers [13]. This difference should correspond to different characteristics of the generated ablation noise.

Previous investigations of the ablation noise [8–12] were performed with condenser microphones limited to a bandwidth of 200 kHz. The bandwidth limitation reduces the potential of the technique, because one would expect the acoustic signal to contain frequency components of up to 1 MHz and beyond due to the short duration of the laser pulses used for ablation. We therefore extended the detectable frequency range to 1 MHz by use of a piezoelectric airborne transducer. This technique makes it possible to detect the high frequency components generated by shock wave emission and fast ejection of ablation products. We performed Schlieren laser flash photography in order to get an understanding of the kinetics of the ablation process generating the ablation noise. The investigations indicated that most of the ablation takes place during the beginning of the laser pulse. The corresponding acoustic measurements also demonstrated that the maximum pressure amplitudes are generated during this initial phase. By evaluating the initial phase of the acoustic signal we could show that the acoustic energy is a tissue-specific parameter suitable to discriminate between tissue layers of different water content like necrotic and vital tissue.

MATERIALS AND METHODS

Irradiated Samples

We irradiated gelatin samples with different water content as well as excised specimens of burned skin. Burned skin was modeled using gelatin samples of different water content in order to create reproducible experimental conditions. The water content of vital epidermis is 70% [14,15]. Burn injuries cause an increase in capillary permeability with subsequent plasma leakage into the interstitial space, resulting in excessive edema formation in the remaining vital tissue [16]. The total water content of the skin increases by about 12% [17] as measured 24 hours post burn for full thickness skin samples including both necrotic and vital tissue components. The above value is an average over the full thickness of the skin. The water content in the dried and shrunk nectrotic tissue layer is considerably less than the water content in the underlying vital tissue. We chose gelatin samples containing 90% water to model the edematous vital tissue and samples with 70% water content to model the necrotic tissue. The actual water content of necrotic tissue may be even lower than 70%. Besides single layered samples we used stacked gelatin samples with a top layer of 70% and bottom layer of 90% water content as a model for burned skin. The stacked gelatin layers were separated by a film of acrylic spray lacquer (Dupli-Color, Vogelsang, Hassmersheim, Germany) to inhibit water diffusion between the layers. The samples were stored in a refrigerator until use.

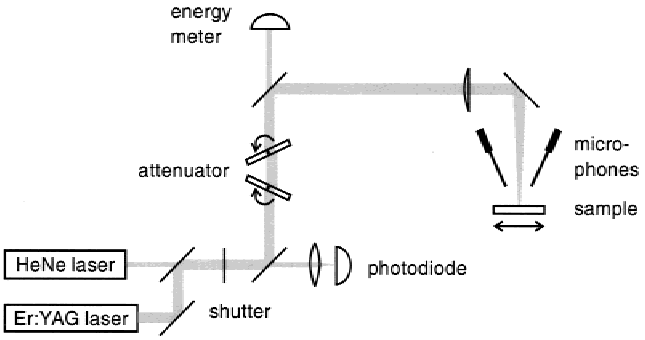

Fig. 1. Experimental setup for acoustic on-line monitoring of Er:YAG laser ablation.

The model experiments with tissue phantoms were followed by in vitro measurements on freshly excised second degree burned human skin. The full thickness samples were excised during conventional burn surgery and irradiated within 60 minutes after excision. To avoid desiccation, the specimens were stored in a closed plastic bag at 7°C until use.

Laser Irradiation

We used a free-running Er:YAG laser (LISA Laser Products, Katlenburg, Germany) delivering pulses with a maximum pulse energy of 400 mJ at 300 μs pulse duration. The laser was operated at 10 Hz repetition rate. The Er:YAG laser radiation was combined with an He:Ne aiming laser beam using a dichroic mirror (Fig. 1). The laser energy could be varied by means of two rotatable quartz plates, which were mechanically coupled to rotate in opposite direction. This allowed the variation of the energy without changing the pump energy, which would otherwise alter the pulse duration and beam profile. The pulse energy was measured by using a pyroelectric probe (DigiRad P-444, Terahertz Technologies, Oriskany, NY). The temporal laser pulse shape was detected by a GaAs photodiode (EG&G Judson J125AP-R02M, Montgomeryville, PA; rise time 10 ns) connected to an oscilloscope (Tektronix, Wilsonville, DE, TDS-540). The laser beam was focused onto the sample with a 100 mm planoconvex lens giving rise to a spot diameter of 450 μm.

Laser Flash Photography

Laser flash photography of the ablation dynamics was performed using a dark field Schlieren arrangement (Fig. 2). The Schlieren technique was employed for the detection of shock waves and of gaseous ablation products, which are hard to identify with conventional photography. For illumination we used 6-ns pulses from a dye laser (Rhodamin 6G) pumped by a frequency doubled Nd:YAG laser. The dye laser was employed to achieve spectral broadening leading to reduced speckle. Spatial frequency filtering for the detection of phase objects was performed using a wire blocking out the image of a slit located in the illumination beam path. Wire and slit are orientated perpendicular to the sample surface giving a maximum sensitivity to refractive index changes parallel to the sample surface. Photographs with different delays between the Er:YAG laser pulse and the illuminating laser pulse were taken on Kodak TMAX 400 film (Eastman Kodak, Rochester, NY).

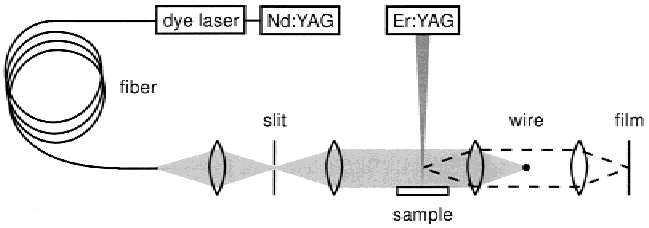

Fig. 2. Dark field Schlieren arrangement for laser flash photography.

Acoustic Investigations

The ablation noise was detected using a condenser microphone (Bruel & Kjaer, Naerum, Denmark, 4138) with a bandwidth of 6.5 Hz–200 kHz (–5 dB), and a piezoelectric airborne transducer (PCB, 132A42) with a bandwidth of 5 kHz–1 MHz. The microphone signals were recorded with a digital oscilloscope (Tektronix TDS 540) and read out into a PC to perform signal analysis. Hanning time window FFT analysis was implemented using IDL (Interactive Data Language). All measurements were performed simultaneously with both microphones. The microphones were oriented under an angle of 35° to the optical axis of the laser beam at a distance of 30 mm from the sample surface.

RESULTS

Laser Flash Photography

Figure 3 shows the Er:YAG laser ablation of gelatin at various times after the first laser spike. The times when the photographs were taken with respect to the laser pulse are indicated in Figure 4. The ablation was performed using a radiant exposures of 21 J/cm^2 (ablation threshold for skin 1.2 J/cm^2 [18]).

The picture taken 4 μs after the first laser spike shows the emission of a hemispherical

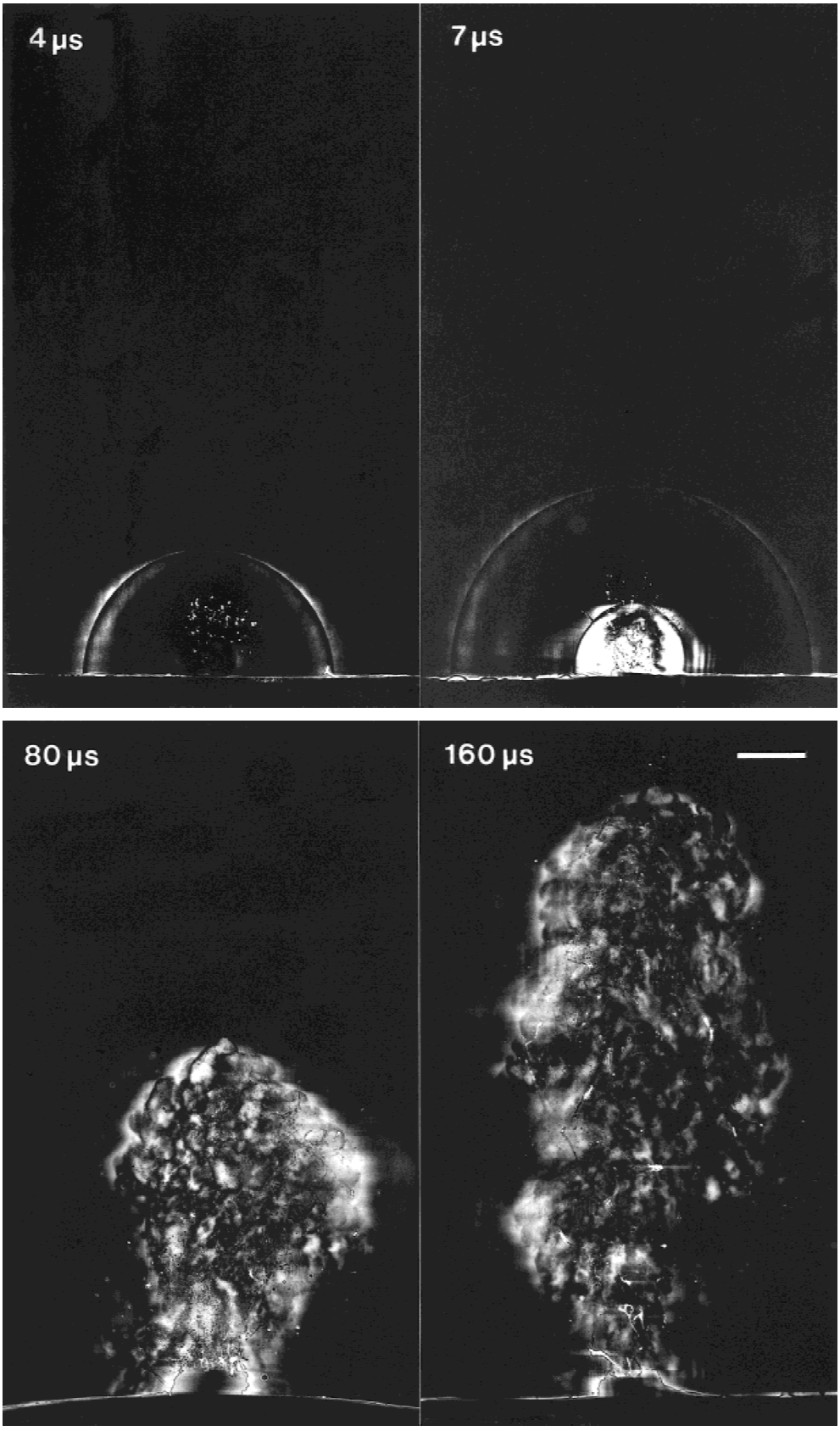

Fig. 3. Laser flash photographs of Er:YAG laser ablation of gelatin with 90% water content. The photographs were taken with a dark field Schlieren technique at various times after the first laser spike (laser pulse energy 33 mJ, focus diameter 450 µm, radiant exposure 21 J/cm^2). The length of the scale corresponds to 1 mm.

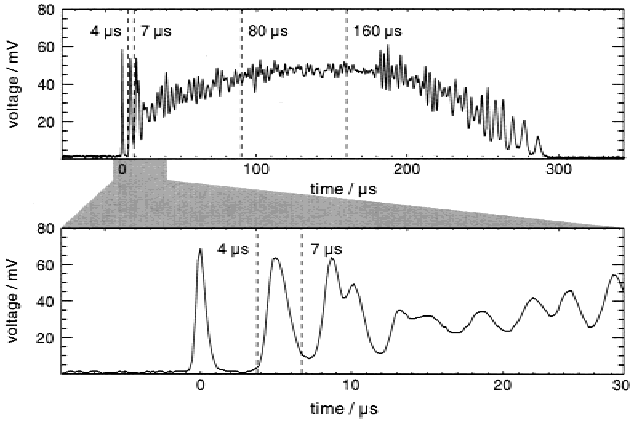

Fig. 4. Typical laser pulse shape used for the gelatin ablation shown in Figure 3 together with the times when the photographs were taken. The pulse shape belongs to the event photographed 7 µs after the initial laser spike.

shock wave as well as the ejection of water vapor and some ablation products out of the ruptured sample surface. After 7 µs the first shock wave has propagated radially and a second shock wave has been generated. Figure 4 demonstrates that the two shock waves correspond to the first two spikes of the Er:YAG laser pulse. The amount of ablation products ejected after the second laser spike is larger than after the first spike. After 80 µs an ablation plume consisting of water vapor, water droplets, and gelatin fragments has been formed. A hump is visible at the sample surface, which probably consists of a wall formed around the crater from which the material is ejected. At later times (160 µs) the ablation plume continues to expand vertically, but the particle and vapor density near the sample surface decrease. This decrease occurs already at a time when the incident laser power is still close to its maximum value (see Fig. 4).

Acoustic Signals

Figures 5(a,b) show a comparison of the acoustic signals that were simultaneously measured with the condenser microphone and the piezoelectric transducer during Er:YAG laser ablation of gelatin. The maximum pressure values measured by the piezoelectric transducer are about a factor of 4.5 higher than the values detected with the condenser microphone. The piezoelectric transducer reveals a decay of the pressure amplitude after about 50 µs that is hardly visible with the condenser microphone. The frequency spectra of both acoustic signals are presented in Figure 5(c). They show that the ablation noise

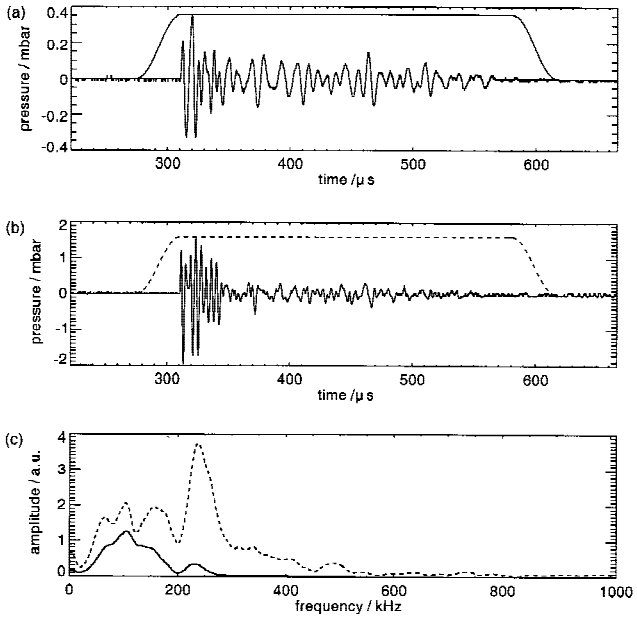

Fig. 5. Er:YAG laser ablation of gelatin with 90% water content. (**a**) Condenser microphone, (**b**) piezoelectric transducer, (**c**) frequency spectra for the time windows shown in (a) and (b). Pulse energy 100 mJ. The signal of the piezoelectric transducer contains considerable more information than that of the condenser microphone.

contains frequency components beyond 600 kHz, which are only detectable with the piezoelectric transducer. Because the information content of the piezoelectric transducer signals is considerably larger than that of the condenser microphone, we shall in the following focus on the signal analysis for this transducer. We shall restrict the evaluation to the initial part of the laser pulse, because Figure 5(b) shows that the ablation noise is mainly produced during the first 50 µs of the pulse.

Figure 6 shows a comparison of the initial part of the laser pulse and the acoustic signal. To facilitate comparison the signals are aligned for coincidence of their fifth maximum. The peaks in the signals show a one to one correlation indicating that each individual laser spike causes a separate ablation event leading to the generation of a pressure pulse. The acoustic transients produced by the first two laser spikes appear shifted to earlier times with respect to the laser spikes. These transients are shock waves (Fig. 3) traveling faster than the speed of sound because of their high pressure amplitude, whereas the later transients are acoustic waves.

The correlation between laser spikes and peaks of the acoustic signal is also reflected in the spectral domain (Fig. 7). We performed time win-

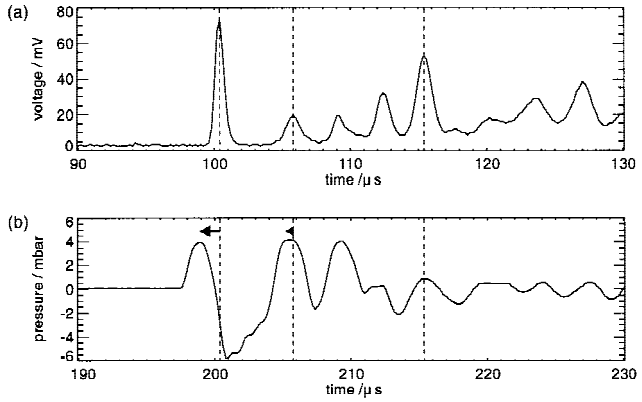

Fig. 6. Initial part of the laser pulse (**a**) and the acoustic signal measured with a piezoelectric transducer (**b**) during ablation of gelatin with 90% water content. The signals are aligned for coincidence of the fifth maximum of the acoustic signal with the fifth laser spike.

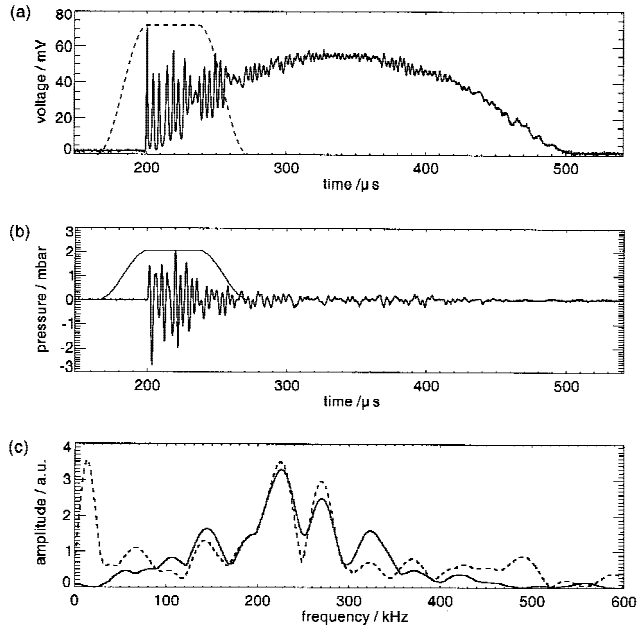

Fig. 7. Time window FFT analysis of the laser pulse and of an acoustic signal during Er:YAG laser ablation of gelatin. (**a**) laser pulse, (**b**) piezoelectric transducer signal, and (**c**) frequency spectra for the time windows shown in (a) and (b). Pulse energy 100 mJ. The peaks in the acoustic spectrum are strongly correlated with the time constants in the spiking sequence.

dow FFT analysis of the initial part of the laser pulse [Fig. 7(a)] and of the corresponding transducer signal [Fig. 7(b)]. Figure 7(c) shows that the maxima of both spectra coincide in the frequency range between 130 and 350 kHz. At lower and higher frequencies no correlation was observed.

Tissue Discrimination

We used the acoustic energy $E = \int p^2(t)\, dt$ as a characteristic parameter for tissue discrimination. The acoustic signals where integrated over the first 50 µs of the laser pulse where they exhibit the highest amplitudes and thus the highest tissue specificity is expected [Fig. 5(b)]. The acoustic energy was normalized to the laser pulse energy incident on the sample during the same period of time to take account of the variations of the pulse energy.

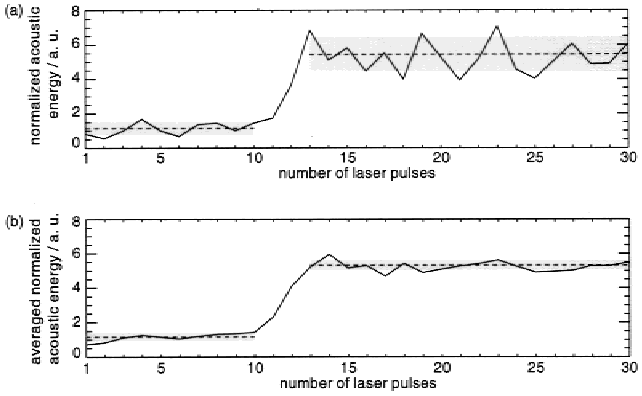

Fig. 8. Er:YAG laser ablation of a stacked gelatin sample (top layer 70%, bottom layer 90% water content). (**a**) Acoustic energy of the first 50 µs of the piezoeletric transducer signal normalized to the laser pulse energy in this time window. (**b**) Normalized acoustic energy averaged over three successive laser pulses. Normalized acoustic energy rises from a lower to a higher level when the ablation front proceeds into the layer with higher water content. Dashed lines and shaded areas show mean and standard deviation of the acoustic energy levels.

For the gelatin samples of 70% and 90% water content, we obtained values of 1.39 ± 0.65 and 3.35 ± 1.44 (arb. units) when the acoustic energy was determined with the piezoelectric transducer (mean and standard deviation). The respective values for the condenser microphone were 0.62 ± 0.46 and 1.77 ± 1.14 (arb. units). The values were averaged over 30 laser pulses, with each pulse aimed at a new unexposed ablation site. The averaged acoustic energy is, hence, three times larger for the sample with the higher water content. The difference can be used for sample discrimination in the case of the piezoelectric transducer, because the error intervals do not overlap. For the condenser microphone however, the error intervals do overlap, probably because of the limited bandwidth of the transducer. The mean values for both microphones differ statistically significantly ($P = 0.99$ in Student t-test).

Figure 8(a) shows a representative result of the experiments performed with stacked gelatin samples. The normalized acoustic energy is plotted as a function of the number of applied laser pulses. The acoustic energy increases from a

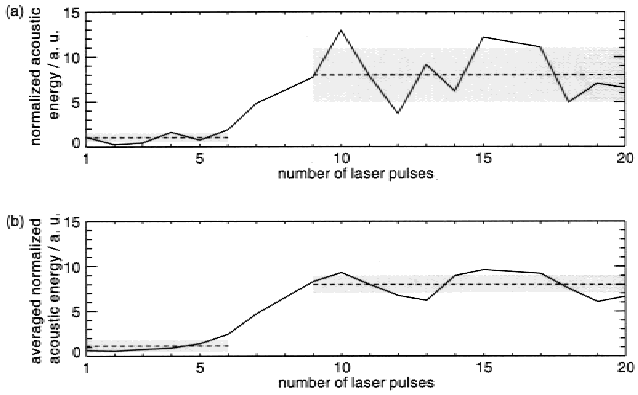

Fig. 9. Er:YAG laser ablation of second degree burned skin (female breast). (**a**) Acoustic energy of the first 50 μs of the piezoelectric transducer signal normalized to the laser pulse energy in this time window. (**b**) Normalized acoustic energy averaged over three successive laser pulses. Normalized acoustic energy rises from a lower to a higher level corresponding to the two necrotic and vital tissue. Dashed lines and shaded areas show mean and standard deviation of the acoustic energy levels.

lower to a higher level when the ablation front propagates into the sample. Microscopic observations confirmed that the two energy levels are correlated to the two sample layers with different water content.

The energy levels in Figure 8(a) differ by a factor of 4.6. For the ablation of 10 different sites on the same sample the ratio of the energy levels was 5.0 ± 1.3, and the energy levels were reproducible with a standard deviation of 20%.

A representative result for the ablation of second degree burned skin is shown in Figure 9. The normalized acoustic energy increases by a factor of 11 when the ablation front proceeds through the transition zone between necrotic and vital tissue. The factor varied between 6 and 12 when the experiment was repeated at 10 different ablation sites on the same tissue sample.

Additional experiments on homogeneous gelatin samples and excised vital skin showed that the formation of an ablation crater had no significant influence on the acoustic energy. This demonstrates that geometrical factors are not responsible for the increase of the acoustic energy during the pulse series presented in Figures 8 and 9.

DISCUSSION

Laser Flash Photography

The photographic investigations give an insight into the generation process of the ablation noise (Fig. 3). The pictures taken 4 μs and 7 μs after the first laser spike show the emission of shock waves that are correlated to the first and second laser spike, as shown in Figure 4. Later on in the laser pulse, shock waves are not observed any more. The shock waves are generated by the fast compression of the air in front of the plume of water vapor and ablation products that are rapidly ejected from the ruptured sample surface. The duration of the first two laser spikes in Figure 4 (FWHM 1μs) is shorter than the thermal relaxation time t_r of water, which is the main chromophore of the sample ($t_r = 1/(\kappa\,\alpha^2) = 4.4$ μs [19], assuming an absorption coefficient$^{\alpha}$ = 12,700 cm^{-1} [20] and a thermal diffusivity $\kappa \approx 1.42 \times 10^{-3}$ cm^2/s [21]). The high energy density in the superficial sample layer caused by the thermal confinement conditions gives rise to high ejection velocities essential for the generation of the supersonic shock waves.

After the explosive onset of the ablation process, the spikes become slightly longer and are superimposed on a steadily increasing background intensity (Fig. 4). The reduced modulation of the laser power leads to a smaller modulation of the energy density in the sample and thus to a more continuous ablation process. As a consequence, the amplitude of the acoustic signal decreases to less than 1/5 of the maximum value within about 50 seconds, although the incident laser power is still very high (Fig. 7).

The reduced modulation of the laser power may also contribute to the decrease of the particle density near the ablation site observed in the picture taken 160 μs after the beginning of the pulse (Fig. 3). Another factor contributing to the decrease of the ablation efficiency is the partial absorption of incident laser light by the ablation plume. The absorption is mainly due to the liquid and solid particles in the plume; the water vapor hardly absorbs at 2.94 μm (α = 0.014 cm^{-1} for 1 bar at 500 °K [22], the absorption maximum is located at 2.7 μm [23]).

The ablation plume does not only impair the energy deposition into the sample, but also distorts the acoustic transients traveling away from the ablation site, because the turbulent flow in the plume creates zones with different density (Fig. 3) and, hence, acoustic impedance. Both the distortion of the acoustic signal and its reduced amplitude lead to a loss of tissue specificity. The highest degree of tissue-specific information is contained in the initial part of the acoustic signal (approx. 50 μs), and only this part of the signal is therefore used for tissue differentiation.

Acoustic Investigations

Microphone comparison. The microphone used for the detection of the ablation noise should have a sensitivity and bandwidth large enough to resolve the tissue-specific components of the acoustic signals. Figure 5(c) shows that frequencies beyond 600 kHz are contained in the ablation noise. These high frequency components are generated by the fast ablation dynamics during the initial phase of the ablation process leading to shock wave emission. They could only be detected by the piezoelectric transducer but not by the condenser microphone with a bandwidth of only 200 kHz.

Figure 6 suggests that for a complete temporal and amplitude resolution of the shock waves containing the highest frequency components of the ablation noise, the transducer bandwidth needs to be even larger than 1 MHz. The first shock wave travels at a considerably higher speed than the second shock wave (Fig. 6). This indicates that the amplitude of the first shock wave is larger, as would also be expected from the intensity ratio of the first two laser spikes. The difference in the amplitude is, however, not visible in the measured acoustic signal. This observation can be explained if the duration of the first shock wave is shorter than that of the second shock wave, and both are shorter than the rise time of the microphone. In this case, the amplitude of both shock waves would be detected too low [24], but the error would be larger for the first, stronger shock wave. The limitation of the microphone bandwidth thus leads to a distortion of the relative amplitude of successive peaks in the initial high frequency acoustic signal. An extension of the microphone bandwidth beyond 1 MHz would be desirable.

To estimate the range for a useful bandwidth extension, one needs to consider the strong damping of high frequency acoustic waves in air ($\sim f^2$ [25]). The propagation distance where the amplitude is damped to 1/e is 8.7 cm at 1 MHz, and 8.7 mm at 3 MHz [25]. At a distance of 30 mm from the ablation site, where the microphone was placed in our study, frequencies of up to 2 MHz should be detectable. Further high frequency components are permanently generated by nonlinear effects during shock wave propagation. These components, however, have no strong correlation to the tissue-specific generation process of the ablation noise and are therefore only of minor interest for an on-line monitoring.

Time domain analysis. The duration of the acoustic signals was found to be similar to the laser pulse duration. The highest pressure amplitudes were generated during the first 50 μs of the laser pulse by explosive evaporation events giving rise to shock wave emission. Later on, a more continues ablation process took place, which generated only small pressure amplitudes.

During the first 30 μs of the laser pulse, each laser spike generated an individual acoustic transient (Fig. 6). A one to one correlation between the Er:YAG laser spikes and the ejection of ablation particles was also observed by other researchers using a pump probe technique [26,27]. In spite of the correlation between laser spikes and acoustic signal, a direct evaluation of the acoustic signal in the time domain does not seem to be very promising for a tissue discrimination because of the large pulse to pulse variations of the laser pulse shape. A normalization of the pressure amplitudes by the laser pulse shape cannot easily solve this problem, because the acoustic signal is distorted in an unknown way by the limited bandwidth of the transducer.

Frequency domain analysis. The strong correlation between the laser pulse shape and the acoustic signal during the initial phase of the ablation process leads to a coincidence of the maxima of the spectra of the laser pulse and the acoustic signal in the range between 130 and 350 kHz [Fig. 7(c)]. This means that most features of the acoustic spectrum are not tissue-specific but just a reflection of the spiking sequence in the laser pulse. We could not identify tissue-specific properties of the spectral amplitudes in any particular frequency range. This is not very surprising because the variations of the laser pulse shape impair the spectral analysis in a similar way as already discussed for the time domain analysis. To overcome these limitations, we focused on the analysis of integral properties of the acoustic signal, particularly the acoustic energy.

Tissue Discrimination

The results of our model experiments using gelatin samples of different water content demonstrate that the normalized acoustic energy is a suitable parameter to discriminate between samples of 70% and 90% water content. The acoustic energy increases with an increasing water content of the sample. This observation can be explained by the dependence of the acoustic energy on the volumetric energy density of the sound source, which is determined by the optical

penetration depth of the laser radiation. In the case of infrared laser ablation, the optical penetration depth is a function of the tissue water content. A high water content causes a larger acoustic energy because the laser energy is confined in a small tissue volume producing a more violent ablation. It is not yet fully understood, however, why a difference in the sample water content of only 20% leads to a threefold increase of the normalized acoustic energy, which is much higher than the increase of 20% one would expect taking only the different optical penetration depth into account. A possible reason may be given by different mechanical properties of the samples.

A tissue discrimination by analysis of *absolute values* of the normalized acoustic energy is not practicable because the water content and thus the acoustic energy varies within a burn area, and the acoustic energy depends also on other parameters beside the tissue water content (for example, the distance between microphone and ablation site). The transition between different layers can, however, be identified by monitoring the *relative change* of the acoustic energy during ablation.

The change of the acoustic energy must be larger than the statistical pulse to pulse variations in order to define a threshold value demarcating a tissue boundary. To overcome the statistical uncertainties, the normalized acoustic energy was averaged over three consecutive shots. Figures 8(b) and 9(b) show that this results in a considerably standard deviation of the energy values corresponding to each layer. A disadvantage of the averaging technique is the broadening of the transition zone between the two levels.

The width of the transition zone between the two levels of the acoustic energy for gelatin ablation (Fig. 8) is caused by inhomogeneities in the laser beam profile. Nonuniform ablation leads to contributions of both gelatin types to the characteristics of the acoustic signal when the ablation front passes the boundary between the layers. Top hat beam profiles should lead to a more homogeneous tissue ablation and thus to a faster increase of the acoustic energy. This would improve the spatial selectivity of the on-line monitoring. In the case of burned skin ablation (Fig. 9) the transition zone is moreover a consequence of the finite width of the transition zone between the necrotic and vital tissue layers.

The maximum possible depth resolution of the acoustic on-line control is given by the ablation depth of the laser if the transition zone between nectrotic and vital tissue is very sharp. In most practical cases, however, the transition zone is thicker than the single shot ablation depth, and the depth resolution is given by the thickness of the transition zone.

The normalized acoustic energy increased by a factor of 5 in the case of the stacked gelatin sample (Fig. 8) whereas it increased by a factor of 6 to 12 for the burned tissue (Fig. 9). These results suggest that the difference between the water content of necrotic and vital tissue is larger than the difference of 20% between the gelatin layers. It is unlikely that the edematous tissue contains much more than 90% water, but it seems quite reasonable that the water content of the necrotic tissue is less than 70%, i.e., less then the hydration of vital epidermis.

Measurements during gelatin ablation using the condenser microphone showed overlapping error intervals for the averaged acoustic energy of the samples with 70% and 90% water content. These results confirm that a significant part of the tissue-specific information is contained in the high frequency components of the ablation noise and that large bandwidth transducers are essential for the discrimination between soft tissues.

The present investigations are a first step towards an on-line control of laser necrectomy. Further studies have to investigate the influence of the kind of burn injury and its treatment prior to laser ablation on the water content of the tissue layers and the acoustic signal in order to determine reliable thresholds for the discrimination between necrotic and vital tissue. These data sets should allow the design of on-line controlled scanning laser systems for fast laser necrectomy of large area burns.

CONCLUSIONS

Our investigations showed that a discrimination between necrotic and vital tissue during infrared laser ablation of burned skin is possible through an evaluation of the normalized acoustic energy of the ablation noise. Large bandwidth acoustic transducers (1 MHz) are essential for the detection of the tissue-specific high frequency components, which are generated during the initial phase of the ablation process.

ACKNOWLEDGMENTS

The authors appreciate helpful discussions with J. Noack and thank W. Eisenbeiß for many

stimulating discussions and for providing the tissue samples.

REFERENCES

1. Jackson DM, Stone FRCS, Stone PA. Tangential excision and grafting of burns. Brit J Plast Surg 1972;25:416–426.
2. Green HA, Domankevitz Y, Nishioka NS. Pulsed carbon dioxide laser ablation of burned skin: In vitro and in vivo analysis. Lasers Surg Med 1990;10:476–484.
3. Green HA, Burd EE, Nishioka NS, Compton CC. Skin graft take and healing following 193-nm excimer, continuous-wave carbon dioxide (CO_2), pulsed CO_2, or pulsed Holmium:YAG laser ablation of graft bed. Arch Dermatol 1993;129:979–988.
4. Green HA, Burd E, Nishioka NS. Middermal wound healing. Arch Dermatol 1992;128:639–645.
5. Leung WP, Tam AC. Noncontact monitoring of laser ablation using a miniature piezoelectric probe to detect photoacoustic pulses in air. Appl Phys Lett 1992;60(1):23–25.
6. Ladislav G, Mozina J. Acoustic in situ monitoring of excimer laser ablation of different ceramics. Applied Surface Science 1993;69:370–375.
7. Stauter C, Gerard P, Fontaine J, Engel T. Laser ablation acoustical monitoring. Appl Surf Sci 1997;109/110:174–178.
8. Bende T, Matallana M, Kleffner B, Jean B. Noncontact photoacoustic spectroscopy during photoablation: a step towards the smart laser? Ophthalmic Technologies V, SPIE 1995;2293:111–119.
9. Jean B, Bende T, Matallana M. Noncontact photoacoustic spectroscopy during photoablation with a 193-nm excimer laser. German J Ophthalmol 1993;2:404–408.
10. Altshuler GB, Belikov AV, Boiko KN, Erofeev AV, Vitiaz IV. Acoustic response of hard dental tissues to pulsed laser action. Dental Applications of Lasers, SPIE 1993;2080:97–103.
11. Altshuler GB, Belinkov AV, Erofeev AV, Scrypnik AV. Research of hard tooth tissue acoustic response under contact YAG:Er laser radiation processing. Laser Applications in Medicine and Dentistry, SPIE 1996;2922:228–232.
12. Grad L, Mozina J, Sustercic D, Funduk N, Skaleric U, Lukac M, Cencic S, Nemes K. Optoacoustic studies of Er:YAG laser ablation in hard dental tissue. Laser Surgery: Advanced characterization, Therapeutics, and systems IV, SPIE 1994;2128:456–465.
13. Demling RH, Mazess RB, Witt RM, Wolberg WH. The study of burn wound edema using dichromatic absorptiometry. J Trauma 1978;18(2):124–128.
14. Warner RR, Mark C, Myers BS, Taylor DA. Electron probe analysis of human skin: Determination of the water concentration profile. J Invest Dermatol 1988;90:218–224.
15. Knox FS, Wachtel TL, McCahan GR, Knapp SC. Thermal properties calculated from measured water content as a function of depth in porcine skin. Burns 1986;12(8):556–562.
16. Arturson G. Pathophysiology of the burn wound. Ann Chirug Gynaecol 1980;69:178–190.
17. Matsuda T, Tanaka H, Shimazaki S, Matsuda H, Abcarian H, Reyes H, Hanumadass M. High-dose vitamin C therapy for extensive deep dermal burns. Burns 1992; 18(2):127–131.
18. Hibst R, Kaufmann R. Vergleich verschiedener Mittelinfrarot-Laser für die Ablation der Haut. Lasermedizin 1995;11:19–26.
19. Carslaw HS, Jaeger JC. Conduction of heat in solids. Oxford: Clarendon Press; 1947.
20. Hale GM, Querry MR. Optical constants of water in the 200-nm to 200-μm wavelength region. Appl Opt 1973; 12(3):555–563.
21. Welch AJ, van Gemert MCJ, editors. Optical-Thermal Response of Laser-Irradiated Tissue. Lasers, Photonics, and Electro-Optics. New York: Plenum Press; 1995.
22. Young JS. Evaluation of nonisothermal band model for H_2O J Quant Spectrosc Radiat Transfer 1977;18:29–45.
23. Wolfe WL, Zissis GJ. The infrared handbook, chapter 5. Third edition. Washington, DC: Office of Naval Research; 1989.
24. Vogel A, Lauterborn W. Acoustic transient generation by laser-produced cavitation bubbles near solid boundaries. J Acoust Soc Am 1988;84(2):719–731.
25. Kuttruff H. Physik und Technik des Ultraschalls. Hirzel; 1988. p 199.
26. Walsh JT, Deutsch TF. Measurement of Er:YAG laser ablation plume dynamics. Appl Phys B 1991;52:217–224.
27. Frenz M, Zweig AD, Romano V, Weber HP, Chapliev NI, Silenoc AS. Dynamics in laser cutting of soft tissue. Laser-Tissue Interaction, SPIE 1990;1202:22–33.